Molecules and Cells

MAPK3 at the Autism-Linked Human 16p11.2 Locus Influences Precise Synaptic Target Selection at *Drosophila* Larval Neuromuscular Junctions

Sang Mee Park[1], Hae Ryoun Park[1,2], and Ji Hye Lee[1,2,*]

[1]Department of Oral Pathology and BK21Plus Project, School of Dentistry, Pusan National University, Yangsan 50612, Korea, [2]Institute of Translational Dental Sciences, Pusan National University, Yangsan 50612, Korea
*Correspondence: jihyelee@pusan.ac.kr
http://dx.doi.org/10.14348/molcells.2017.2307
www.molcells.org

Proper synaptic function in neural circuits requires precise pairings between correct pre- and post-synaptic partners. Errors in this process may underlie development of neuropsychiatric disorders, such as autism spectrum disorder (ASD). Development of ASD can be influenced by genetic factors, including copy number variations (CNVs). In this study, we focused on a CNV occurring at the 16p11.2 locus in the human genome and investigated potential defects in synaptic connectivity caused by reduced activities of genes located in this region at *Drosophila* larval neuromuscular junctions, a well-established model synapse with stereotypic synaptic structures. A mutation of *rolled*, a *Drosophila* homolog of human *mitogen-activated protein kinase 3* (*MAPK3*) at the 16p11.2 locus, caused ectopic innervation of axonal branches and their abnormal defasciculation. The specificity of these phenotypes was confirmed by expression of wild-type *rolled* in the mutant background. Albeit to a lesser extent, we also observed ectopic innervation patterns in mutants defective in Cdk2, $G\alpha_q$, and Gp93, all of which were expected to interact with Rolled MAPK3. A further genetic analysis in double heterozygous combinations revealed a synergistic interaction between *rolled* and *Gp93*. In addition, results from RT-qPCR analyses indicated consistently reduced *rolled* mRNA levels in *Cdk2*, *$G\alpha_q$*, and *Gp93* mutants. Taken together, these data suggest a central role of MAPK3 in regulating the precise targeting of presynaptic axons to proper postsynaptic targets, a critical step that may be altered significantly in ASD.

Keywords: 16p11.2, autism, copy number variations, *Drosophila*, MAPK3

INTRODUCTION

Precise coordination between correct pre- and post-synaptic partners in the nervous system is important for its normal functions in both vertebrates and invertebrates. Synaptic contacts between neurons are established during the embryonic period as differentiating neurons navigate through the extracellular environment and locate their appropriate targets (see Christensen et al., 2013 for a recent review). As a presynaptic neuron approaches its postsynaptic target, an individual presynaptic axon is defasciculated from an axon bundle consisting of multiple axons that travel together toward their specific target to form a synapse.

A number of studies have been performed in the last few decades to unravel the identities of proteins that are critical for specific coordination between pre- and post-synaptic partners (Christensen et al., 2013). Recently, it has been suggested that dysfunction in these critical components may underlie the pathogenesis of various neuropsychiatric diseases, including schizophrenia, bipolar disorder, and autism spectrum disorder (ASD), affecting a significant fraction of the world's population. For example, schizophrenia-associated mutations in reelin (RELN) and disrupted in schizophrenia1

Received 13 December, 2016; revised 22 January, 2017; accepted 23 January, 2017; published online 15 February, 2017

eISSN: 0219-1032

(DISC1) can cause defects in neuronal migration (Kamiya et al., 2005), dendritic organization, and remodeling of synapses (Arnold, 1999). In addition, protocadherin 12 (PCDH12) linked to schizophrenia (Gregorio et al., 2009) has been implicated in neuronal differentiation and synaptogenesis (John et al., 2015). In line with these findings, another report has suggested the possibility of neuropsychiatric diseases associated with genetic perturbations in the cell adhesion molecule (CAM) pathway, including NRXN1, CNTNAP, and CASK (Redies et al., 2012).

Among the major neuropsychiatric disorders, ASD is characterized by defects in social communication and language development as well as restricted and repetitive behaviors that develops by the age of three (Abrahams and Geschwind, 2008; Reiss et al., 1986; Zoghbi and Bear, 2012). The clinical aspects for diagnosis and behavioral treatments of ASD have been mostly considered in the earlier studies, but a greater attention is now being given to genetic abnormalities that could potentially contribute to the development of ASD. Due to its complex nature, as suggested by multi-layered genetic interactions (see Bourgeron, 2015 for a recent review), it is very difficult to delineate individual candidate genes and relevant molecular pathways of which defects may underlie the pathogenesis of ASD. Recent attempts to elucidate such complex genetic contributions to ASD have employed population- and genome-based analyses, including linkage studies and genomic-wide association studies. As a result, novel genetic components have been identified, ranging from individual genes to chromosomal regions encompassing multiple genes (Bourgeron, 2015). Important outcomes of these genome-based studies in patients with ASD include significant correlations with repetitive deletion or duplication of specific chromosomal regions that leads to changes in the copy number of genes enclosed in the region, called copy number variations (CNVs). Indeed, CNVs at multiple chromosomal loci, including 2p16.3, 3p26.c, 15q11-q13, 16p11.2, and 22q13.33, appear to have strong associations with ASD (Sebat et al., 2007).

Among these CNV loci, frequent deletion or duplication events in the 16p11.2 region have been linked to ASD and schizophrenia in a series of familial studies (Kumar et al., 2008; Marshall et al., 2008; Portmann et al., 2014; Weiss et al., 2008). Furthermore, these events have been estimated to be responsible for up to 1% of ASD cases according to a previous study (5 out of 512 children) (Weiss et al., 2008). The 16p11.2 locus includes 27 annotated genes within an approximately 500Kb segment (Horev et al., 2011; Pucilowska et al., 2015), many of which have been implicated in neural development (Golzio et al., 2012; Kumar et al., 2008; Miyazaki et al., 2006). A recent study using a zebrafish model has demonstrated significant structural abnormalities induced by defects in zebrafish genes homologous to human counterparts at the 16p11.2 locus, including a change in brain size and eye structure as well as formation of abnormal axonal tracts (Blaker-Lee et al., 2012). In addition, dysfunction of extracellular signal-regulated kinase 1 (ERK1) encoded by *mitogen-activated protein kinase 3* (*MAPK3*) located within this region leads to changes in brain size and cortical cytoarchitecture in a murine model system (Pucilowska et al., 2015). Taken together, these data suggest critical roles of ASD-linked genes localized at the 16p11.2 locus in precise regulation of neural development. Despite these recent efforts, the specific contributions of individual genes to the development of neural circuits remain poorly understood.

We have recently conducted a RNAi-based genetic screen using *Drosophila melanogaster* to analyze contributions of individual genes in the 16p11.2 region to synaptic morphology (Park et al., 2016). The *Drosophila* neuromuscular junction (NMJ) is one of the most well characterized glutamatergic model systems that provides a unique opportunity to systematically study structural and functional abnormalities induced by genetic perturbations at well-defined and stereotypic synapses (Atwood et al., 1993; Hoang and Chiba, 2001; Johansen et al., 1989; Menon et al., 2013). Taking advantage of this system, we monitored the presence of aberrant synaptic architecture, such as errors in presynaptic nerve innervation and formation of synaptic boutons. As a result, we found abnormal innervation patterns and premature defasciculation of presynaptic motor axons in mutants defective in *Drosophila rolled* (*rl*), a gene homologous to human *MAPK3*. Further analyses revealed significant genetic interactions between *rl* and other genes, of which protein products were expected to interact with Rolled MAPK3 according to a proteomic study (Friedman et al., 2011), and a central role of *rl* in this genetic network. Together with previous reports using zebrafish and murine models, our results provide another line of evidence to support the idea that Rolled MAPK3 plays an important role in regulating neuronal architecture and the hypothesis that such structural defects during development may underlie the pathogenesis of ASD.

MATERIALS AND METHODS

Fly stocks

All crosses and stocks were raised on standard media at 24℃ with 45%-60% humidity. The Canton-S and w^{1118} strains were used as wildtype (WT) controls. All fly stocks used in our study obtained from Bloomington Drosophila Stock Center include: 1) rl^{1} for *rolled* (*rl*); 2) *w*; Cdk2*^{3}*/TM3, Sb*^{1} *P{35UZ}2*, y^{1} *sc* v*^{1}*; P{TRiP.GL00162}attP2* and y^{1} *sc* v*^{1}*; P{TRiP. GL00611}attP40* for *cyclin-dependent kinase 2 (Cdk2)*; 3) cn^{1} $G\alpha_{q}{}^{1}$ and *w*; P{w[+mC]=UAS-Gα*$_{q}$*. dsRNA.1f1}2/CyO, P{w[+mC]=ActGFP}JMR1* for *G-protein αlpha-q subunit* ($G\alpha_{q}$); 4) y^{1} w^{67c23}*; P{EPgy2}Gp93*^{EY06213} and y^{1} *sc* v*^{1}*; P{TRiP. HMS01334}attP2* for *glycoprotein 93* (*Gp93*). The *elav*^{c155}*-GAL4* and *mef2-GAL4* drivers based upon the GAL4-UAS system (Brand and Perrimon, 1993) were used for expression of neuron- and muscle-specific dsRNA (RNAi) lines, respectively. y^{1} v^{1}*; P{CaryP}attP2* and y^{1} v^{1}*; P{CaryP}attP40* were used as controls, along with *UAS-rl*$^{+}$ (w^{1118}*; P{UAS-rl.K}2A*) as a transgenic line carrying the WT gene. Whenever possible, we used multiple RNAi lines and mutant alleles for each gene to confirm the effect of RNA interference and mutations and combined the results from multiple variants since they showed similar trends, albeit slight differences in the severity of their phenotypes.

Immunohistochemistry

Male third instar larvae were dissected in 1X Phosphate-buffered saline (PBS) and prepared for immunofluorescent staining, as previously described (Lee and Wu, 2010). The morphology of neuromuscular junctions (NMJs) was visualized with Alexa 594-conjugated goat anti-HRP antibody (1:250; Jackson ImmunoResearch Laboratories, USA). For direct comparison of absolute FasII density among *rl, Cdk2, $G\alpha_q$* and *Gp93* mutants as well as WT, the samples were simultaneously treated for immunofluorescent staining in the same tube and incubated with anti-FasII (1D4) antibody (at 1:100; Developmental Studies Hybridoma Bank, USA) followed by Alexa 488-conjugated goat anti-mouse antibody (at 1:400; Jackson ImmunoResearch Laboratories).

Image analysis

The Z-stack images of body-wall muscles 12 (M12) and 13 (M13) were obtained from the abdominal segments A2 - A3 using a confocal microscope (Zeiss, LSM700; Carl Zeiss, Germany) and processed with ZEN software (Carl Zeiss). The pattern of axonal targeting was monitored in M13 that is normally innervated with type Ib, Is and II axon branches, but not with type III axons. These types of axon branches innervate target muscles by forming synaptic boutons of different sizes and shapes (Atwood et al., 1993). The presence of synaptic boutons originating from type III axons was counted as an ectopic innervation of type III axons at a specific synapse. The frequency or the ratio of ectopic type III axon innervations at M13 NMJs (the number of M13 NMJs with ectopic type III synaptic boutons over total number of NMJs examined) was then calculated for each genotype for further analyses. In addition, the defasciculation status of axonal bundles was monitored at the boundary of M13 and M12. The premature defasciculation was then defined as early separation of axon fibers within a single axon bundle before it made contact with M12. The frequency or the ratio of premature defasciculation (the number of NMJs with premature defasciculation over total number of NMJs examined) was then calculated for each genotype for further analyses.

For direct comparison of FasII immunoreactivities, the same confocal scanning protocols were applied to all samples that were treated together in the same tube during an immunostaining procedure. The FasII density was then measured as pixel intensity from at least six type Ib synaptic boutons innervating muscle 12 and connecting axon braches using the ImageJ package (NIH, USA).

qRT-PCR analysis

Total RNA was extracted from heads of WT and mutant flies using RNeasy Mini Kit (QIAGEN Korea Ltd., Korea), followed by synthesis of cDNA from 2 μg of extracted RNA using QuantiTect Reverse Transcription Kit (QIAGEN). The real-time reverse transcription qPCR reaction (RT-qPCR) was performed using the SYBR Green qPCR master mix (Enzynomics, Korea) in a 96-well plate. The reaction cycles were initiated with a denaturation step (95°C for 10 min), followed by 40 cycles consisting of denaturation (95°C for 15 s), annealing (60°C for 20 s) and extension steps (72°C for 30 s). The RT-qPCR analysis was conducted using Applied Biosystems 7500 Real-Time PCR system (USA). The mRNA levels of *GAPDH* were measured as a reference for comparison. The primer sets used for RT-qPCR analyses include: forward 5′-GCAAGGGTGCGTCCTATGAT-3′ and reverse 5′-AGAGTGTGGGTGGGTAGTGT-3′ for *GAPDH*; forward 5′-CATGGTTGTGTCTGCGGATG-3′ and 5′-GCTTATGGCATGGTTGTGTCTG-3′ and reverse 5′-AAGTTT-GGTGTTCAAAGGGCG-3′ and 5′-TTGGTGTTCAAAGGGC-GATA-3′ for two independent *rolled* sets; forward 5′- CAACCAGGTGGGATTAGGAA-3′ and reverse 5′-TAACG- CCCGGACAGTATTTG-3′ for total FasII (Beck et al., 2012). Each RT-qPCR reaction was performed in triplicate. The relative gene expression level compared to control was calculated using the $2^{-\Delta\Delta Ct}$ method (Livak and Schmittgen, 2001). The results were summarized from at least three independent experiments.

Statistical analyses

To compare the proportional differences in ectopic axon branches between two groups, the data were categorized in the 2 × 2 contingency tables (with phenotypes *vs.* without phenotypes in two groups) and subjected to Fisher's exact test. The RT-qPCR data from multiple genotypes were compared using one-way Analysis of Variance (ANOVA) followed by Tukey's post-hoc test. *P* values less than 0.05 were considered significant.

RESULTS

Abnormal patterns of motor axon innervation and defasciculation in *rolled* mutants

CNVs at the 16p11.2 locus have been implicated in familial cases of ASD (Kumar et al., 2008; Marshall et al., 2008; Portmann et al., 2014; Weiss et al., 2008). However, the identities of the genes responsible for the pathological features of ASD linked to these CNVs are not well understood in experimental settings. To systematically investigate the roles of individual human genes in this region, we recently performed an RNAi-based genetic screen using *Drosophila melanogaster* (Park et al., 2016). The most striking abnormalities in this screen, including multiple and ectopic innervations of presynaptic motor axons into postsynaptic body-wall muscles, were detected in larvae expressing double-stranded RNA targeting *rl*, a gene homologous to human *MAPK3* at the 16p11.2 locus (Supplementary Fig. S1). To further confirm that these phenotypes were specifically induced by the loss of Rolled MAPK3, a mutational analysis was performed with a loss-of-function allele of the *rl* mutants (rl^{1}). Consistent with the phenotypes induced by an RNAi-based knockdown approach, a mutation in *rl MAPK3* resulted in two distinct structural abnormalities at larval NMJs formed in the abdominal body-wall muscles (Fig. 1).

When innervation patterns of presynaptic motor axons were examined in muscles 13 (M13) and 12 (M12) of the abdominal body-wall musculature in WT and *rl* mutants, we found aberrant innervations of type III axons in *rl* larvae (Fig. 1A, middle panel). Unlike other motor axons transducing glutamatergic signals, the synaptic terminals of type III axons contain neuropeptides (Gorczyca et al., 1993; Gramates and Budnik, 1999). Their postsynaptic target in WT animals is

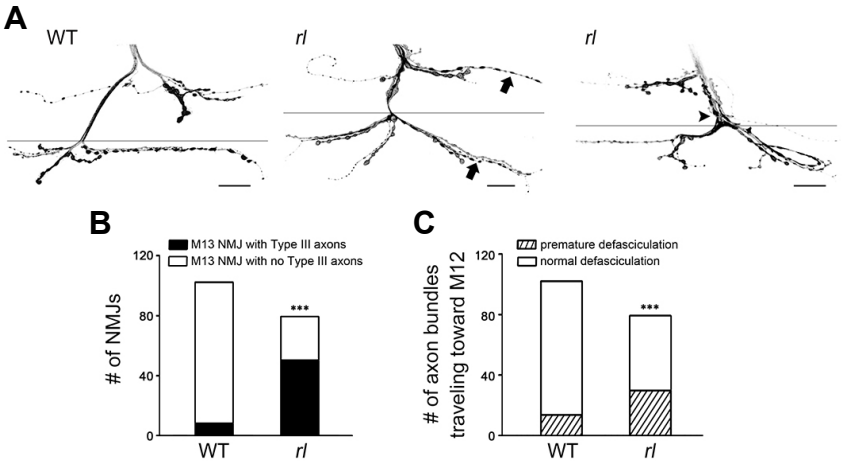

Fig. 1. Aberrant innervation patterns of type III axons and premature axonal defasciculation in *rolled MAPK3* mutants. (A) A mutation of *rolled* (or *rl*) cause morphologic changes at *Drosophila* larval NMJs, including ectopic targeting of type III axons to muscle 13 (arrow) and premature defasciculation of axon bundles at the boundary of muscles 13 and 12 (arrowheads), both of which are rarely detected in WT animals. Scale bar, 20 μm. (B, C) The frequency of ectopic type III axons (B) and premature axonal defasciculation (C) is shown for WT and *rl* larvae. The number of NMJs examined: WT, 102 and *rl*, 79. ***, $P < 0.001$, Fisher's exact test between WT and *rl*.

extremely restricted, mostly with a sole innervation into M12, but not in any other the body-wall musculature (Hoang and Chiba, 2001) (Supplementary Fig. S2; see also Fig. 1A, left panel). In contrast, *rl* mutants often displayed innervations of type III axons into M13 and M12, as evidenced by the presence of type III synaptic boutons of a distinct shape and size (Fig. 1A, middle panel, arrows). To quantify the severity of this targeting error, we counted the frequency of ectopic innervation by type III axons in M13 of WT and *rl* mutants. As shown in Fig. 1B, the number of M13 NMJs with ectopic type III axons was significantly higher in *rl* mutants. In fact, the majority of *rl* NMJs displayed additional innervation of type III axons (Fig. 1B for the pooled data, 7.84% (8 of 102) for WT vs. 63.29% (50 of 79) for *rl*, $P < 0.001$ for WT vs. *rl*; see Supplementary Table S1A).

In addition to such an aberrant innervation pattern in *rl* mutants, we observed premature defasciculation of presynaptic axon bundles near M12. The majority of axon bundles containing individual motor axons targeted to M12 remained fasciculated in WT until they traveled underneath M13 and finally reached the surface of M12 (Fig. 1A, left panel; see also Supplementary Fig. S2). However, we found that a significant fraction of these axons in *rl* mutants exited the bundles and were separated from each other before they made contact with M12 (Fig. 1A, right panel, arrowhead; Fig. 1C for the pooled data, 13.73% (14 of 102) for WT vs. 37.97% (30 of 79) for *rl*, $P < 0.001$ for WT vs. *rl*; see Supplementary Table S1B). This is an interesting parallel to a previous study demonstrating reduced and disorganized axonal tracts induced by loss of MAPK3 in zebrafish embryos (Blaker-Lee et al., 2012). Thus, our results strongly suggest a potential contribution of Rolled MAPK3 to organization of presynaptic axon bundles and their proper targeting to postsynaptic targets.

Defective targeting of type III axons and premature defasciculation rescued with expression of WT Rolled in the mutant background

Abnormal targeting of type III axons and premature defasciculation of axon bundles in *rl* mutants may result from defective MAPK3 signaling in either the pre- or post-synaptic compartment. To delineate the specific contributions of neuronal and muscular MAPK3 to proper targeting of these axons, we performed rescue experiments with pre- or post-synaptic expression of WT *rl* (*UAS-rl*$^{+}$) in the *rl* mutant background using the GAL4-UAS system (Brand and Perrimon, 1993). The *elav*^{C155}- and *mef2-GAL4* drivers were used for specific expression of *rl*$^{+}$ in neuronal and muscular compartments, respectively. As a control, we first examined the effect of *rl* overexpression in the WT background. Larvae presynaptically overexpressing WT *rl* (*elav*^{C155}*-GAL4→UAS-rl*$^{+}$) did not differ from control groups (either *elav*^{C155}*-GAL4* or *UAS-rl*$^{+}$ alone) in their innervation patterns of type III axons at M13 NMJs or in the defasciculation profiles of axon bundles at the border of M12 (Supplementary Fig. S3).

Then, we examined the effect of *rl* overexpression in the mutant background. As expected, a transgenic construct of WT *rl* alone (*UAS-rl*$^{+}$) in the absence of a proper GAL4 driver was insufficient to induce any significant changes in synaptic abnormalities detected in the *rl* mutant background (Fig. 2A, top panels). The fraction of animals with aberrant type III innervation into M13 and premature axonal defasciculation before M12 remained high in *rl* mutants with no GAL4 driver (Fig. 2B for type III axons in M13, $P < 0.001$ for WT vs. *rl*^{1}, *UAS-rl*$^{+}$; Fig. 2C for premature defasciculation, $P < 0.001$ for WT vs. *rl*^{1}, *UAS-rl*$^{+}$). However, neuronal expression of WT *rl* in mutants led to a significant decrease in the fraction of type III axons targeted to M13, almost to the WT level (Fig. 2A, bottom left; Fig. 2B, $P < 0.01$ for *rl*^{1}, *UAS-rl*$^{+}$ vs. *elav*^{C155}*-GAL4/Y; rl*^{1}, *UAS-rl*$^{+}$). On the other hand, the degree of rescue in premature defasciculation defects by neuronal expression of WT *rl* failed to reach statistical significance, albeit a tendency to diminish the mutant phenotype (Fig. 2C). In case of muscular expression of WT *rl*, the frequency of aberrant innervation of type III axons into M13 remained higher in mutants than that in the WT control (Fig. 2B, $P < 0.05$ for WT vs. *rl*^{1}, *UAS-rl*$^{+}$*; mef2-GAL4/+*), but mutant phenotypes

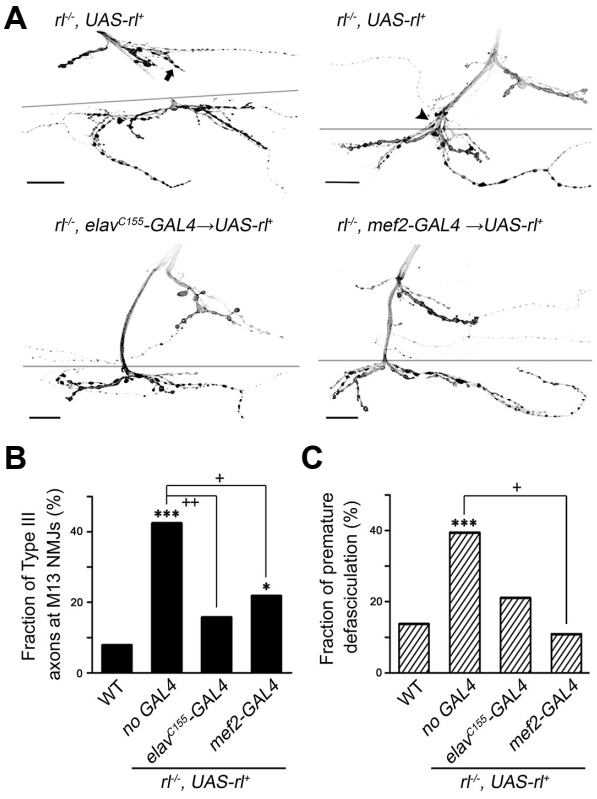

Fig. 2. Phenotypic rescue of axon targeting and defasciculation errors by expression of wild-type *rolled* in presynaptic motor neurons and postsynaptic muscles. (A) The *rl* mutant phenotypes, including ectopic targeting of type III axons to muscle 13 (arrow) and premature axonal defasciculation (arrowhead), are rescued by neuron- and muscle-specific expression of WT Rolled (rl^{+}). The $elav^{C155}$- and *mef2-GAL4* lines were used for neuron- and muscle-specific expression of a transgenic rl^{+} construct under the influence of *UAS* element, respectively. Scale bar, 20 μm. (B, C) The fraction of ectopic type III axons (B) and premature axonal defasciculation (C) is shown for each genotype. The fraction of mutant phenotypes observed in animals containing only a transgenic rl^{+} construct in the mutant background (*rl, UAS-rl*$^{+}$) serves as a control, along with WT. The data from WT in Fig. 1 are duplicated for comparisons. The number of NMJs examined for each genotype: WT, 102; *rl, UAS-rl*$^{+}$, (no GAL4) 33; $elav^{C155}$-*GAL4* → *UAS-rl*$^{+}$, 57; *mef2-GAL4* → *UAS-rl*$^{+}$, 55. ***, $P < 0.001$ for Fisher's exact test between WT and the genotype indicated. $^{++}$, $P < 0.01$ and, $^{+}$, $P < 0.05$ for Fisher's exact test between *rl, UAS-rl*$^{+}$ (no GAL4) and the genotype indicated.

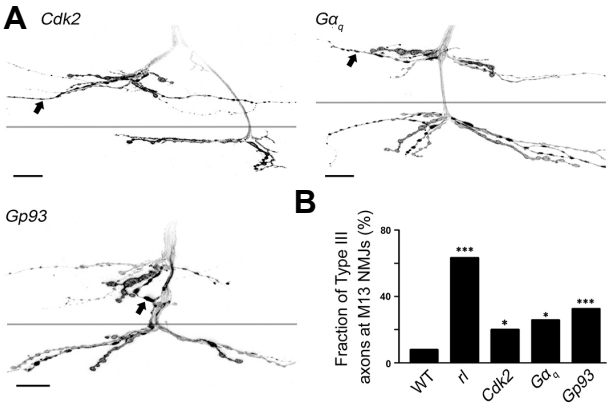

Fig. 3. Aberrant innervation patterns of type III axons observed in mutants defective in MAPK3-associated proteins. (A) Ectopic targeting of type III axons to muscle 13 (arrows), a phenotype observed in *rl* mutants, is also detected in mutants defective in *Cdk2*, $G\alpha_q$ and *Gp93*. Scale bar, 20 μm. (B) The fraction of aberrant type III innervation patterns is shown for each genotype. The data from WT and *rl* groups in Fig. 1B are duplicated for comparisons. The number of NMJs examined: WT, 102; *rl*, 79; *Cdk2*, 35; $G\alpha_q$, 35; *Gp93*, 40. ***, $P < 0.001$ and $^{*}P < 0.05$ for Fisher's exact test between WT and the genotype indicated.

in both innervation and fasciculation patterns were significantly attenuated (Fig. 2A, bottom right; Figs. 2B and 2C, $P < 0.05$ for rl^{1}, *UAS-rl*$^{+}$ vs. rl^{1}, *UAS-rl*$^{+}$; *mef2-GAL4/+*), with a more striking effect on premature defasciculation (Fig. 2C).

Taken together, our results indicate significant contributions of both neuronal and muscular Rolled MAPK3 in finding a proper target for type III axons and tightly controlling axonal defasciculation. These data also suggest differential molecular mechanisms implicated in the regulation of proper synaptic connectivity and defasciculation events of axon bundles, both of which may involve MAPK3 activities.

Genetic interactions between MAPK3 and functionally linked proteins involved in aberrant targeting of type III axons

A previous proteomic analysis has suggested strong functional links between Rolled MAPK3 and diverse classes of proteins, including cyclin-dependent kinase 2 (Cdk2), G-protein alpha-q ($G\alpha_q$), and glycoprotein 93 (Gp93) (Friedman et al., 2011). It is possible that the activities of these functional networks coordinate proper targeting and defasciculation of motor axons. If that is the case, dysfunction of these network components other than Rolled MAPK3 would also lead to similar abnormalities observed in *rl* mutants. To test this idea, we performed genetic analyses using mutants defective in Cdk2, $G\alpha_q$, and Gp93 and examined their synaptic morphology (Fig. 3). Due to the higher ratio of mutant phenotypes, we focused on an analysis of aberrant innervation patterns of type III axons in M13 of these mutants.

Importantly, ectopic type III axons in M13 were frequently detected in *Cdk2*, $G\alpha_q$, and *Gp93* mutants (Fig. 3). To further confirm specific contributions of these molecules to the target selection process, synaptic morphology was monitored in transgenic animals with a RNAi-based knockdown of each gene (Supplementary Table S2). Significant changes in innervation patterns were only evident upon expression of dsRNA constructs against *Cdk2*, but not $G\alpha_q$ or *Gp93* (Supplementary Table S2). However, we observed a tendency for more frequent ectopic type III axons in some of these dsR-

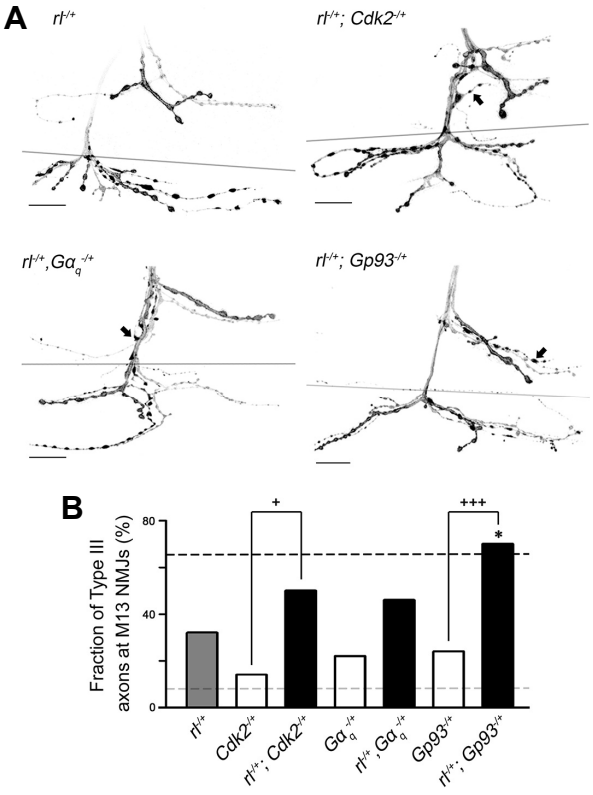

Fig. 4. Genetic interactions between *rolled* and genes encoding MAPK3-associated proteins. (A) Double heterozygous larvae for both *rl* and one of the associated genes among *Cdk2*, $G\alpha_q$ and *Gp93* display frequently mistargeted type III axons in muscle 13 (arrows). Scale bar, 20 μm. (B) The fraction of aberrant type III innervation patterns is shown for single and double heterozygous combinations indicated. Upper (black) and lower (light gray) dashed lines represent the fraction observed in *rl* homozygous mutants and WT, respectively. The number of NMJs examined: $rl^{/+}$, 31; $Cdk2^{-/+}$, 35; $rl^{/+}$; $Cdk2^{-/+}$, 20; $G\alpha_q^{-/+}$, 36; $rl^{/+}$, $Cdk2^{-/+}$, 24; $Gp93^{-/+}$, 34; $rl^{/+}$; $Gp93^{-/+}$, 20. *, $P < 0.05$ for Fisher's exact test between *rl* single heterozygous ($rl^{/+}$) and corresponding double heterozygous mutants indicated. $^{+++}$, $P < 0.001$ and $^{+}$, $P < 0.05$ for Fisher's exact test between single and double heterozygous pairs indicated.

NA-expressing animals (Supplementary Table S2), supporting, in part, the possibility that these genes may play important roles in regulating proper targeting of motor axons, together with *rl*. It should be noted that the proportions of *Cdk2*, $G\alpha_q$ and *Gp93* mutants with abnormal innervation patterns were significantly lower than that of *rl* mutants (Fig. 3B), suggesting a dominant contribution of Rolled MAPK3 within these protein networks to proper synaptic target selection.

Our results demonstrating similar mutational phenotypes in mutants defective in Rolled MAPK3 as well as Cdk2, $G\alpha_q$, and Gp93 suggest that they may interact with each other and thus participate in similar signaling pathways. We tested this idea by monitoring the presence of genetic interactions between *rl* and other genes among *Cdk2*, $G\alpha_q$, and *Gp93* in double heterozygous combinations. When single heterozygous animals were analyzed for their phenotypes in type III innervation patterns, we found that *rl* heterozygotes ($rl^{/+}$) showed a slightly higher ratio of ectopic type III axons in M13. A similar, but lesser degree of increase in the ratio was also detected in $G\alpha_q$ and *Gp93* single heterozygotes ($G\alpha_q^{-/+}$ and $Gp93^{-/+}$) (Fig. 4B). Despite these unexpected increases in single heterozygous animals, some double heterozygous combinations, specifically $rl^{/+}$; $Cdk2^{-/+}$ and $rl^{/+}$; $Gp93^{-/+}$, displayed an apparent increase in the ratio of ectopic type III innervation (Figs. 4A and 4B, $P < 0.05$ for $Cdk2^{-/+}$ *vs.* $rl^{/+}$; $Cdk2^{-/+}$ and $P < 0.001$ for $Gp93^{-/+}$ *vs.* $rl^{/+}$; $Gp93^{-/+}$). In case of *rl* and *Gp93*, the ectopic innervation ratio measured in double heterozygous mutants ($rl^{/+}$; $Gp93^{-/+}$) was much higher than that in either single heterozygote ($rl^{/+}$ *or* $Gp93^{-/+}$) or the combined ratio of the two heterozygotes (Fig. 4B), suggesting a clear synergistic interaction between *rl* and *Gp93*.

Transcriptional regulation of Rolled MAPK3 in mutants with ectopic innervation patterns of type III axons

Our results described above demonstrate a critical role of Rolled MAPK3 and relevant protein networks in regulating the proper selection of synaptic targets. Based upon the phenotypic similarities in mutants and the presence of genetic interactions, it is plausible that reduced activity of Rolled MAPK3 may underlie expression of the consistent mutant phenotypes we observed. We verified this idea by analyzing the level of the *rl* transcript in *Cdk2*, $G\alpha_q$, and *Gp93* mutants with a RT-qPCR assay. WT and *rl* animals were included in the set as a negative and positive control, respectively. When the mRNA levels of the reference housekeeping gene *glyceraldehyde-3-phosphate dehydrogenase* and *rl* were measured using two independent *rl* primers (sets 1 and 2), consistent and significant downregulation of *rl* transcripts was evident in *Cdk2*, $G\alpha_q$, and *Gp93* mutants, similar to the phenotype observed in *rl* mutants (Figs. 5A and 5B, $P < 0.001$ for WT vs. *rl*, $G\alpha_q$ or *Gp93* and $P < 0.01$ for WT vs. *Cdk2*). These results parallel the potential genetic interactions indicated by the enhanced mutant phenotypes of ectopic type III axons in the double heterozygous combinations (Fig. 4B), further confirming a central role for Rolled MAPK3 in regulating innervation patterns of type III axons.

It has been suggested that Rolled MAPK3 regulates the expression of fasciclin II (FasII) at *Drosophila* larval NMJs (Koh et al., 2002). FasII, a *Drosophila* homolog of human neuronal cell adhesion molecule (NCAM), plays a critical role in regulating various aspects of synaptic development, including axonal pathfinding and fasciculation as well as synaptic growth, via its homophilic interactions between pre- and post-synaptic compartments (Lin et al., 1994; Schuster et al., 1996a; 1996b). Based on these findings, we examined whether the *fasII* transcript level was altered in mutants using a primer specific to total *fasII* RNA (Beck et al., 2012). Among those screened, the $G\alpha_q$ and *Gp93* mutants displayed a slight, but significant downregulation of total *fasII* transcripts (Fig. 5C; $P < 0.05$ and $P < 0.01$, WT vs. $G\alpha_q$ and *Gp93*, respectively). However, we failed to detect transcriptional changes in *fasII* induced by an *rl* mutation (Fig. 5C),

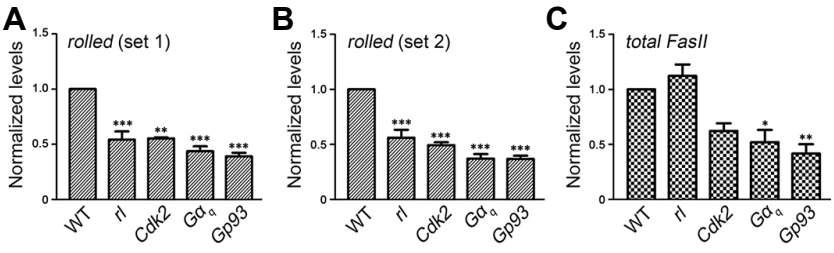

Fig. 5. Transcriptional regulation of *rolled MAPK3* and *fasII* in *Cdk2*, $G\alpha_q$ and *Gp93* mutants. (A-C) The relative levels of mRNA estimated from qRT-PCR analyses with two independent *rl* primers (A, B) and a single fasII primer (C) are shown for each genotype. The level of mRNA in WT animals is used as a control to normalize the values measured from mutants. The levels of each mRNA are measured from at least three independent sets of triplicate samples. ***, $P < 0.001$, **, $P < 0.01$ and *, $P < 0.05$ for one-way ANOVA between WT and the genotype indicated, followed by Tukey's post-hoc test for pair-wise comparisons.

inconsistent with a previous report suggesting a functional link between Rolled MAPK3 and FasII (Koh et al., 2002). Furthermore, direct comparisons of FasII immunoreactivity at larval NMJs did not yield noticeable differences in its distribution among the mutants screened (Supplementary Table S3). Taken together, these results demonstrating discrepancies in transcriptional regulation of *fasII* among mutants with similar structural abnormalities suggest a minimal contribution by FasII to Rolled MAPK3-associated protein networks and the presence of unknown molecular mechanisms responsible for ensuring proper selection of synaptic partners via Rolled MAPK3-dependent pathways.

DISCUSSION

Recent studies on ASD have revealed an important link to CNVs at multiple genomic loci (Sebat et al., 2007). In the present study, we investigated the roles of individual genes at the 16p11.2 locus, one of the CNV spots frequently mapped to ASD, in the regulation of synaptic architecture. We took advantage of the stereotypic and identifiable *Drosophila* larval NMJs, a well-established synaptic model system. Our results indicate defects in nerve innervation patterns and fasciculation of axon bundles induced by a mutation in *Drosophila rl* homologous to human *MAPK3* (Fig. 1). Similar phenotypes were observed in mutants defective in other proteins that are expected to functionally interact with MAPK3, including Cdk2, $G\alpha_q$, and Gp93 (Fig. 3). In line with this result, genetic interactions between *rl* and some of these genes were revealed in double heterozygous mutant combinations (Fig. 4). Finally, downregulation of *rl* transcripts was consistently detected in *Cdk2*, $G\alpha_q$, and *Gp93* mutants, almost comparable to reduced transcript levels in *rl* mutants themselves (Fig. 5). Taken together, these results point toward a central role for Rolled MAPK3 in proper targeting of axons and thus selection of synaptic partners via the activity of a MAPK3-associated protein network.

Abnormal neuronal architecture and its implication in neuropsychiatric disorders

Recent multi-directional research efforts have yielded significant advances in our understanding about the pathophysiology of neuropsychiatric disorders, including schizophrenia, major depression and ASD. As a result, greater attention has been given to the potential involvement of structural abnormalities in the nervous system (Amaral et al., 2008; Arnold, 1999). For example, macroscopic post-mortem analyses of the brain from patients with schizophrenia revealed a significant reduction in its volume, particularly in the areas of the posterior superior temporal gyrus, amygdala-hippocampal complex and hippocampus (Steen et al., 2006; Yoshida et al., 2009). In addition to a gross change in brain size, microscopic changes at the level of individual neurons, such as a decrease in the number and volume of dendritic spines, have been reported in the CA3 region of the hippocampus in patients with schizophrenia (Kolomeets et al., 2005). Similar microscopic changes were also evident in patients with a mood disorder (Law et al., 2014), along with a reduced density of pyramidal neurons and glia in the CA regions of the hippocampus (Stockmeier et al., 2004).

In line with these reports, a body of experimental evidences supports the idea that structural abnormalities in the nervous system confer susceptibility to ASD (see Amaral et al., 2008 for a recent review). Indeed, anatomical differences in several neurocognitive networks have been reported in patients with ASD (Ecker et al., 2012), including greater brain size and enhanced neuronal proliferation in the prefrontal cortex as well as disrupted cellular architecture in the cerebellar cortex (Bauman and Kemper, 2005; Courchesne et al., 2011). Furthermore, brain imaging studies have revealed atypical white- and gray-matter connectivity (Ecker et al., 2012), in line with our results demonstrating abnormal synaptic targeting induced by a mutation in the gene located at an ASD-mapped CNV locus. Taken together, these results demonstrate consistent structural abnormalities in patients suffering from neuropsychiatric disorders and provide useful insights into our understanding of their pathophysiology.

The role of MAPK3 in regulation of synaptic connectivity

While a strong association has been suggested between abnormal neuronal architecture and susceptibility to ASD, the underlying molecular networks involving protein-protein interactions remain poorly understood. In this study, we demonstrated abnormal axonal innervation caused by a mutation in *rl/MAPK3* located at the ASD-mapped 16p11.2 locus and revealed a potential protein network that may participate in controlling proper synaptic target selection.

Drosophila MAPK encoded by *rl* is a protein homologous to human ERK1 encoded by *MAPK3* at the 16p11.2 locus (Biggs and Zipursky, 1992). ERK1 is a serine/threonine kinase

that shares approximately 84% of its sequence with ERK2, another ERK isoform (Boulton and Cobb, 1991; Boulton et al., 1991). ERK1/2 is involved in various aspects of neural development, ranging from neurogenesis to synaptic plasticity underlying learning and memory (Sweatt, 2001). Loss of ERK1/2 activity leads to alterations in the cortical lamina composition along with abnormal neuronal morphology in the cortex and dentate gyrus in mice (Pucilowska et al., 2015; Vithayathil et al., 2015). The expression of *Drosophila* MAPK3 encoded by *rl* has also been reported previously in synaptic boutons at larval NMJs, where it interacts with other synaptic proteins, including FasII, to regulate the number of synaptic boutons (Ko et al., 2002). Studies in murine models and patients with ASD have revealed abnormal upregulation of ERK1/2 signaling activities associated with significant changes in neuronal migration, synapse formation, and maturation of dendritic spines, further confirming a critical role of MAPK in neural development.

In our study, we present a novel phenotype of altered synaptic architecture, including ectopic targeting of presynaptic axons to unnatural postsynaptic partners and early defasciculation of commonly traveling axon bundles that are frequently observed following loss of MAPK3 activity in *Drosophila*. Establishment of precise neural connectivity is crucial for maintaining proper function of the nervous system and requires molecular machinery determining synaptic specificity (Christensen et al., 2013; Tessier-Lavigne and Goodman, 1996). Considering the expression of MAPK/ERK at WT synapses and its abnormal regulation observed in ASD patients, we hypothesize that MAPK3 located at the 16p11.2 locus is a part of the cellular signaling pathways responsible for synaptic specificity and thus for establishing proper neural connectivity. If our hypothesis holds true, dysfunction of MAPK3 could cause significant disturbances in circuit connectivity eventually leading to alterations in neural function, thus predisposing individuals to ASD.

MAPK3-associated protein network in regulation of synaptic connectivity

In addition to Rolled MAPK3, our results shown in Fig. 4 suggest contributions of other molecules presumably linked to MAPK3, including Cdk2, $G\alpha_q$, and Gp93 (Friedman et al., 2011), to specific targeting of presynaptic axons. Cdk2 is a serine/threonine kinase that is important for controlling the cell cycle and thus proliferation by modulating the G1/S transition phase (Tsai et al., 1993). When Cdk2 forms a complex with MAPK in the cytoplasm, activation of MAPK induces translocation of this complex into the nucleus, allowing Cdk2 to regulate transition of the cell cycle from the G1 to the S phase in mammalian cells (Blanchard et al., 2000; Wang et al., 2009). However, whether Cdk2 activity is required during neural development other than the stage of neurogenesis remains unclear. Thus, the significance of the functional interaction between MAPK3 and Cdk2 in the regulation of neuronal architecture awaits further investigation.

$G\alpha_q$, a part of the α subunits of G proteins, activates phospholipase Cβ that hydrolyzes PIP_2 and eventually to diacylglycerol and inositol-1,4,5-triphosphate (see Sánchez-Fernández et al., 2014 for a recent review). In addition to a potential correlation between $G\alpha_q$ activity and other neuropsychiatric disorders such as schizophrenia (Levitt et al., 2006), a recent report indicated a significantly altered *Gαq* transcript level in children with ASD (Jacobson et al., 2014). However, apart from the finding that MAPK3 is downstream of $G\alpha_q$ (Sanchez-Fernandez et al., 2014), our knowledge about $G\alpha_q$ signaling-dependent regulation of MAPK3 activity in the nervous system is extremely limited.

Among various proteins that are potentially linked to MAPK3, our genetic analysis indicates an apparent synergistic interaction between *rl* and *Gp93* compared to *Cdk2* and *Gαq* (Fig. 4B). *Drosophila* Gp93 is an ortholog of mammalian Gp96, a heat shock protein that functions as a chaperone responsible for surveillance, and is mostly implicated in carcinogenesis and inflammation (see Ansa-Addo et al., 2016 for a recent review). Gp93 localizes in the growth cone and synaptosome in the rat brain during the early postnatal period (Henry et al., 1999; Li et al., 1992). Assuming that proper selection of synaptic targets and axonal pathfinding requires precise communication between presynaptic growth cones and their natural targets as well as extracellular guidance cues, it is intriguing to speculate that MAPK3 interacts with Gp93 to control target selection processes at synapses.

Despite the differential degrees of genetic interactions between *rl* and its potential partners, our RT-qPCR analysis demonstrated consistent downregulation of *rl* transcripts in all mutants screened. Transcriptional activity of MAPK3 is suppressed when cells are placed under growth arrest or hypoxic conditions (Hernandez et al., 2004). At this moment, it remains elusive whether such transcriptional suppression is correlated with the activities of MAPK3-related protein network described above or with the process of synaptic formation via selection of proper targets. Further studies will be required to elucidate the molecular mechanisms that induce transcriptional regulation of MAPK3 during synaptic development.

Molecular targets regulated by the MAPK3-related protein network to influence synaptic connectivity

A previous report in *Drosophila* has suggested a MAPK3-dependent regulation of FasII expression at synapses (Koh et al., 2002). Considering the tight association between FasII level and synaptic growth (Schuster et al., 1996a; 1996b) as well as fasciculation of axon tracts (Lin et al., 1994), it is intriguing to hypothesize that loss of MAPK3 activity results in significant changes in the distribution of FasII, subsequently causing aberrant nerve innervation patterns. We have directly tested this idea by monitoring both transcriptional and translational levels of FasII. In contrast to our expectation, we failed to detect any significant changes in *fasII* transcripts or gene products in *rl* mutants, albeit mRNA levels diminished in some mutants affecting potential MAPK3-related network components (Fig. 5C and Supplementary Table S3). Taken together, our results indicate a minor or limited contribution of FasII to aberrant nerve innervation patterns observed in *rl* and other relevant mutants and suggest yet unknown alternative molecular mechanisms underlying MAPK3-dependent synaptic targeting.

Studies on molecular mechanisms of ASD have revealed consistent defects in other synaptic proteins, including Neu-

roligin (NLG), Neurexin (NRX) and SHANK family proteins in ASD patients and animal models (see Chen et al., 2014 for a recent review). Presynaptic NRXs bind to appropriate postsynaptic NLGs to form a trans-synaptic complex and to promote formation and stabilization of the synapse (Chen et al., 2014). A recent report has further confirmed a coordination among NRX, NLG, and Wishful Thinking as important for controlling synaptic architecture and growth at NMJs (Banerjee et al., 2016). In addition to NLG and NRX, SHANK family members are postsynaptic scaffolding proteins that play a critical role in dendritic spine morphogenesis and synaptic plasticity. For example, overexpression and knockdown of SHANK3, one of the SHANK family members, induce changes in dendritic spine morphology in opposite directions (Betancur et al., 2009). Considering their association with ASD, these data together strongly support the idea that synaptic abnormalities induced by dysfunction of NLG, NRX, and SHANK can predispose affected individuals to ASD. However, it should be noted that altered synapse morphology caused by the loss of NLG, NRX, and SHANK is qualitatively different from the aberrant nerve innervation and defasciculation patterns we observed in *rl* mutants. Furthermore, the presence of functional networks that link MAPK3 to NLG-NRX-SHANK has not been confirmed in experimental settings. Therefore, it is unlikely that MAPK3-dependent synaptic targeting process is directly associated with activity of the NLG-NRX-SHANK protein complex. Further studies are necesssary to completely rule out this possibility. Alternatively, unknown and novel molecular mechanisms other than NLG, NRX and SHANK may be activated by the MAPK3-associated protein complex to fine tune the selection of synaptic partners during development. Future studies employing genome-wide or proteomic approaches will shed new light on how synaptic targeting is precisely regulated in a MAPK3-dependent manner.

In summary, we report that the loss of Rolled MAPK3 located in the ASD-mapped 16p11.2 region induces an error in axon targeting and fasciculation. Similar errors can be detected in mutants defective in other proteins functionally associated with MAPK3, presumably via transcriptional regulation of MAPK3. Our findings provide a unique opportunity to study the contributions of individual genes located at ASD-linked CNV hotspots to the regulation of neuronal architecture, or more specifically, proper synaptic connectivity during development. Taking advantage of the well-defined stereotypic nature of synapses, future studies in *Drosophila* will continue to help to identify novel genetic factors that predispose individuals to ASD.

Note: Supplementary information is available on the Molecules and Cells website (www.molcells.org).

ACKNOWLEDGMENTS

This work was supported by a 2-Year Research Grant of Pusan National University to Ji Hye Lee.

REFERENCES

Abrahams, B.S., and Geschwind, D.H. (2008). Advances in autism genetics: on the threshold of a new neurobiology. Nat. Rev. Genet. *9*, 341-355.

Amaral, D.G., Schumann, C.M., and Nordahl, C.W. (2008). Neuroanatomy of autism. Trends Neurosci. *31*, 137-145.

Ansa-Addo, E.A., Thaxton, J., Hong, F., Wu, B.X., Zhang, Y., Fugle, C.W., Metelli, A., Riesenberg, B., Williams, K., Gewirth, D.T., et al. (2016). Clients and oncogenic roles of molecular chaperone gp96/grp94. Curr. Top Med. Chem. *16*, 2765-2778.

Arnold, S.E. (1999). Neurodevelopmental abnormalities in schizophrenia: insights from neuropathology. Dev. Psychopathol. *11*, 439-456.

Atwood, H., Govind, C., and Wu, C.F. (1993). Differential ultrastructure of synaptic terminals on ventral longitudinal abdominal muscles in *Drosophila* larvae. J. Neurobiol. *24*, 1008-1024.

Banerjee, S., Venkatesan, A., and Bhat, M.A. (2016). Neurexin, Neuroligin and Wishful Thinking coordinate synaptic cytoarchite- cture and growth at neuromuscular junctions. Mol. Cell Neurosci. *78*, 9-24.

Bauman, M.L., and Kemper, T.L. (2005). Neuroanatomic observations of the brain in autism: a review and future directions. Int. J. Dev. Neurosci. *23*, 183-187.

Beck, E.S., Gasque, G., Imlach, W.L., Jiao, W., Choi, B.J., Wu, P.-S., Kraushar, M.L., and McCabe, B.D. (2012). Regulation of Fasciclin II and synaptic terminal development by the splicing factor beag. J. Neurosci. *32*, 7058-7073.

Betancur, C., Sakurai, T., and Buxbaum, J.D. (2009). The emerging role of synaptic cell-adhesion pathways in the pathogenesis of autism spectrum disorders. Trends Neurosci. *32*, 402-412.

Biggs, W.H., and Zipursky, S.L. (1992). Primary structure, expression, and signal-dependent tyrosine phosphorylation of a *Drosophila* homolog of extracellular signal-regulated kinase. Proc. Natl. Acad. Sci. USA *89*, 6295-6299.

Blaker-Lee, A., Gupta, S., McCammon, J.M., De Rienzo, G., and Sive, H. (2012). Zebrafish homologs of genes within 16p11.2, a genomic region associated with brain disorders, are active during brain development, and include two deletion dosage sensor genes. Dis. Model. Mech. *5*, 834-851.

Blanchard, D.A., Mouhamad, S., Auffredou, M.-T., Pesty, A., Bertoglio, J., Leca, G., and Vazquez, A. (2000). Cdk2 associates with MAP kinase in vivo and its nuclear translocation is dependent on MAP kinase activation in IL-2-dependent Kit 225 T lymphocytes. Oncogene *19*, 4184-4189.

Boulton, T.G., and Cobb, M.H. (1991). Identification of multiple extracellular signal-regulated kinases (ERKs) with antipeptide antibodies. Cell Regul. *2*, 357-371.

Boulton, T.G., Nye, S.H., Robbins, D.J., Ip, N.Y., Radziejewska, E., Morgenbesser, S.D., DePinho, R.A., Panayotatos, N., Cobb, M.H., and Yancopoulos, G.D. (1991). ERKs: a family of protein-serine/threonine kinases that are activated and tyrosine phosphorylated in response to insulin and NGF. Cell *65*, 663-675.

Bourgeron, T. (2015). From the genetic architecture to synaptic plasticity in autism spectrum disorder. Nat Rev Neurosci *16*, 551-563.

Brand, A.H., and Perrimon, N. (1993). Targeted gene expression as a means of altering cell fates and generating dominant phenotypes. Development *118*, 401-415.

Chen, J., Yu, S., Fu, Y., and Li, X. (2014). Synaptic proteins and receptors defects in autism spectrum disorders. Front. Cell. Neurosci. *8*, 276.

Christensen, R., Shao, Z., and Colon-Ramos, D.A. (2013). The cell biology of synaptic specificity during development. Curr. Opin. Neurobiol. *23*, 1018-1026.

Courchesne, E., Mouton, P.R., Calhoun, M.E., Semendeferi, K., Ahrens-Barbeau, C., Hallet, M.J., Barnes, C.C., and Pierce, K. (2011). Neuron number and size in prefrontal cortex of children with autism. JAMA *306*, 2001-2010.

Ecker, C., Suckling, J., Deoni, S.C., Lombardo, M.V., Bullmore, E.T., Baron-Cohen, S., Catani, M., Jezzard, P., Barnes, A., Bailey, A.J., et al. (2012). Brain anatomy and its relationship to behavior in adults with autism spectrum disorder: a multicenter magnetic resonance imaging study. Arch. Gen. Psychiatry *69*, 195-209.

Friedman, A.A., Tucker, G., Singh, R., Yan, D., Vinayagam, A., Hu, Y., Binari, R., Hong, P., Sun, X., and Porto, M. (2011). Proteomic and functional genomic landscape of receptor tyrosine kinase and ras to extracellular signal-regulated kinase signaling. Sci. Signal. *4*, rs10.

Golzio, C., Willer, J., Talkowski, M.E., Oh, E.C., Taniguchi, Y., Jacquemont, S., Reymond, A., Sun, M., Sawa, A., and Gusella, J.F. (2012). KCTD13 is a major driver of mirrored neuroanatomical phenotypes of the 16p11. 2 copy number variant. Nature *485*, 363-367.

Gorczyca, M., Augart, C., and Budnik, V. (1993). Insulin-like receptor and insulin-like peptide are localized at neuromuscular junctions in *Drosophila*. J. Neurosci. *13*, 3692-3704.

Gramates, L.S., and Budnik, V. (1999). Assembly and maturation of the *Drosophila* larval neuromuscular junction. Int. Rev. Neurobiol. *43*, 93-117.

Gregorio, S.P., Sallet, P.C., Do, K.A., Lin, E., Gattaz, W.F., and Dias-Neto, E. (2009). Polymorphisms in genes involved in neuro-development may be associated with altered brain morphology in schizophrenia: preliminary evidence. Psychiatry Res *165*, 1-9.

Henry, S., Pfenninger, K.H., Mott, J.L., and Granholm, A.-C. (1999). Anatomical distribution of glycoprotein 93 (gp93) on nerve fibers during rat brain development. Cell Tissue Res. *297*, 67-79.

Hernandez, R., Garcia, F., Encio, I., and De Miguel, C. (2004). Promoter analysis of the human p44 mitogen-activated protein kinase gene (MAPK3): transcriptional repression under nonpro-liferating conditions. Genomics *84*, 222-226.

Hoang, B., and Chiba, A. (2001). Single-cell analysis of *Drosophila* larval neuromuscular synapses. Dev. Biol. *229*, 55-70.

Horev, G., Ellegood, J., Lerch, J.P., Son, Y.-E.E., Muthuswamy, L., Vogel, H., Krieger, A.M., Buja, A., Henkelman, R.M., and Wigler, M. (2011). Dosage-dependent phenotypes in models of 16p11. 2 lesions found in autism. Proc. Natl. Acad. Sci. USA *108*, 17076-17081.

Jacobson, J.D., Ellerbeck, K.A., Kelly, K.A., Fleming, K.K., Jamison, T.R., Coffey, C.W., Smith, C.M., Reese, R.M., and Sands, S.A. (2014). Evidence for alterations in stimulatory G proteins and oxytocin levels in children with autism. Psychoneuroendocrinology *40*, 159-169.

Johansen, J., Halpern, M.E., Johansen, K.M., and Keshishian, H. (1989). Stereotypic morphology of glutamatergic synapses on identified muscle cells of *Drosophila* larvae. J. Neurosci. *9*, 710-725.

John, J.P., Thirunavukkarasu, P., Halahalli, H.N., Purushottam, M., and Jain, S. (2015). A systematic review of the effect of genes mediating neurodevelopment and neurotransmission on brain morphology: Focus on schizophrenia. Neurol. Psychiatry Brain Res. *21*, 1-26.

Kamiya, A., Kubo, K., Tomoda, T., Takaki, M., Youn, R., Ozeki, Y., Sawamura, N., Park, U., Kudo, C., Okawa, M., et al. (2005). A schizophrenia-associated mutation of DISC1 perturbs cerebral cortex development. Nat. Cell Biol. *7*, 1167-1178.

Koh, Y.-H., Gorczyca, M., and Budnik, V. (2002). The Ras1-Mitogen-Activated Protein Kinase Signal Transduction Pathway Regulates Synaptic Plasticity through Fasciclin II-Mediated Cell Adhesion. J. Neurosci. *22*, 2496-2504.

Kolomeets, N.S., Orlovskaya, D.D., Rachmanova, V.I., and Uranova, N.A. (2005). Ultrastructural alterations in hippocampal mossy fiber synapses in schizophrenia: a postmortem morphometric study. Synapse *57*, 47-55.

Kumar, R.A., KaraMohamed, S., Sudi, J., Conrad, D.F., Brune, C., Badner, J.A., Gilliam, T.C., Nowak, N.J., Cook, E.H., and Dobyns, W.B. (2008). Recurrent 16p11. 2 microdeletions in autism. Hum. Mol. Genet. *17*, 628-638.

Law, A.J., Weickert, C.S., Hyde, T.M., Kleinman, J.E., and Harrison, P.J. (2014). Reduced spinophilin but not microtubule-associated protein 2 expression in the hippocampal formation in schizophrenia and mood disorders: molecular evidence for a pathology of dendritic spines. Am. J. Psychiatry 161, 1848-1855.

Lee, J., and Wu, C.F. (2010). Orchestration of stepwise synaptic growth by K^+ and Ca^{2+} channels in *Drosophila*. J. Neurosci. *30*, 15821-15833.

Levitt, P., Ebert, P., Mirnics, K., Nimgaonkar, V.L., and Lewis, D.A. (2006). Making the case for a candidate vulnerability gene in schizophrenia: Convergent evidence for regulator of G-protein signaling 4 (RGS4). Biol. Psychiatry *60*, 534-537.

Li, H., Quiroga, S., and Pfenninger, K.H. (1992). Variable membrane glycoproteins in different growth cone populations. J. Neurosci. *12*, 2393-2402.

Lin, D.M., Fetter, R.D., Kopczynski, C., Grenningloh, G., and Goodman, C.S. (1994). Genetic analysis of Fasciclin II in *Drosophila*: defasciculation, refasciculation, and altered fasciculation. Neuron *13*, 1055-1069.

Livak, K.J., and Schmittgen, T.D. (2001). Analysis of relative gene expression data using real-time quantitative PCR and the $2^{-\Delta\Delta CT}$ method. Methods *25*, 402-408.

Marshall, C.R., Noor, A., Vincent, J.B., Lionel, A.C., Feuk, L., Skaug, J., Shago, M., Moessner, R., Pinto, D., and Ren, Y. (2008). Structural variation of chromosomes in autism spectrum disorder. Am. J. Hum. Genet. *82*, 477-488.

Menon, K.P., Carrillo, R.A., and Zinn, K. (2013). Development and plasticity of the *Drosophila* larval neuromuscular junction. Wiley Interdiscip Rev. Dev. Biol. *2*, 647-670.

Miyazaki, T., Hashimoto, K., Uda, A., Sakagami, H., Nakamura, Y., Saito, S.-y., Nishi, M., Kume, H., Tohgo, A., and Kaneko, I. (2006). Disturbance of cerebellar synaptic maturation in mutant mice lacking BSRPs, a novel brain-specific receptor-like protein family. FEBS Lett. *580*, 4057-4064.

Park, S.M., Littleton, J.T., Park, H.R., and Lee, J.H. (2016). *Drosophila* Homolog of Human KIF22 at the Autism-Linked 16p11.2 Loci influences synaptic connectivity at larval neuromuscular junctions. Exp. Neurobiol. *25*, 33-39.

Portmann, T., Yang, M., Mao, R., Panagiotakos, G., Ellegood, J., Dolen, G., Bader, P.L., Grueter, Brad A., Goold, C., Fisher, E., et al. (2014). Behavioral abnormalities and circuit defects in the basal ganglia of a mouse model of 16p11.2 deletion syndrome. Cell Rep. *7*, 1077-1092.

Pucilowska, J., Vithayathil, J., Tavares, E.J., Kelly, C., Karlo, J.C., and Landreth, G.E. (2015). The 16p11. 2 deletion mouse model of autism exhibits altered cortical progenitor proliferation and brain cytoarchitecture linked to the ERK MAPK pathway. J. Neurosci. *35*, 3190-3200.

Redies, C., Hertel, N., and Hubner, C.A. (2012). Cadherins and neuropsychiatric disorders. Brain Res. *1470*, 130-144.

Reiss, A.L., Feinstein, C., and Rosenbaum, K.N. (1986). Autism and genetic disorders. Schizophrenia Bull. *12*, 724.

Sanchez-Fernandez, G., Cabezudo, S., Garcia-Hoz, C., Beninca, C., Aragay, A.M., Mayor, F., Jr., and Ribas, C. (2014). Galphaq

signalling: the new and the old. Cell Signal. *26*, 833-848.

Schuster, C.M., Davis, G.W., Fetter, R.D., and Goodman, C.S. (1996a). Genetic dissection of structural and functional components of synaptic plasticity. I. Fasciclin II controls synaptic stabilization and growth. Neuron *17*, 641-654.

Schuster, C.M., Davis, G.W., Fetter, R.D., and Goodman, C.S. (1996b). Genetic dissection of structural and functional components of synaptic plasticity. II. Fasciclin II controls presynaptic structural plasticity. Neuron *17*, 655-667.

Sebat, J., Lakshmi, B., Malhotra, D., Troge, J., Lese-Martin, C., Walsh, T., Yamrom, B., Yoon, S., Krasnitz, A., and Kendall, J. (2007). Strong association of *de novo* copy number mutations with autism. Science *316*, 445-449.

Steen, R.G., Mull, C., McClure, R., Hamer, R.M., and Lieberman, J.A. (2006). Brain volume in first-episode schizophrenia: systematic review and meta-analysis of magnetic resonance imaging studies. Br. J. Psychiatry *188*, 510-518.

Stockmeier, C.A., Mahajan, G.J., Konick, L.C., Overholser, J.C., Jurjus, G.J., Meltzer, H.Y., Uylings, H.B.M., Friedman, L., and Rajkowska, G. (2004). Cellular changes in the postmortem hippocampus in major depression. Biol. Psychiatry *56*, 640-650.

Sweatt, J.D. (2001). The neuronal MAP kinase cascade: a biochemical signal integration system subserving synaptic plasticity and memory. J. Neurochem. *76*, 1-10.

Tessier-Lavigne, M., and Goodman, C.S. (1996). The molecular biology of axon guidance. Science *274*, 1123-1133.

Tsai, L.H., Lees, E., Faha, B., Harlow, E., and Riabowol, K. (1993). The cdk2 kinase is required for the G1-to-S transition in mammalian cells. Oncogene *8*, 1593-1602.

Vithayathil, J., Pucilowska, J., Goodnough, L.H., Atit, R.P., and Landreth, G.E. (2015). Dentate gyrus development requires ERK activity to maintain progenitor population and MAPK pathway feedback regulation. J. Neurosci. *35*, 6836-6848.

Wang, B., Gao, Y., Xiao, Z., Chen, B., Han, J., Zhang, J., Wang, X., and Dai, J. (2009). Erk1/2 promotes proliferation and inhibits neuronal differentiation of neural stem cells. Neurosci. Lett. *461*, 252-257.

Weiss, L.A., Shen, Y., Korn, J.M., Arking, D.E., Miller, D.T., Fossdal, R., Saemundsen, E., Stefansson, H., Ferreira, M.A., and Green, T. (2008). Association between microdeletion and microduplication at 16p11. 2 and autism. N Engl. J. Med. *358*, 667-675.

Yoshida, T., McCarley, R.W., Nakamura, M., Lee, K., Koo, M.-S., Bouix, S., Salisbury, D.F., Morra, L., Shenton, M.E., and Niznikiewicz, M.A. (2009). A prospective longitudinal volumetric MRI study of superior temporal gyrus gray matter and amygdala-hippocampal complex in chronic schizophrenia. Schizophrenia Res. *113*, 84-94.

Zoghbi, H.Y., and Bear, M.F. (2012). Synaptic dysfunction in neurodevelopmental disorders associated with autism and intellectual disabilities. Cold Spring Harb Perspect Biol. *4*.